Investigation on Growth, Structure and Characterization of Succinate salt of 8-hydroxyquinoline: An organic NLO Crystal

ARTICLE *in* SPECTROCHIMICA ACTA PART A MOLECULAR AND BIOMOLECULAR SPECTROSCOPY · DECEMBER 2014

Impact Factor: 2.35 · DOI: 10.1016/j.saa.2014.12.093

4 AUTHORS, INCLUDING:

Babu Balraj
Ramakrishna Mission Vidyalaya
15 PUBLICATIONS **24** CITATIONS
SEE PROFILE

K. Anitha --
Madurai Kamaraj University
36 PUBLICATIONS **190** CITATIONS
SEE PROFILE

J. Chandrasekaran
Sri Ramakrishna Mission Vidyalaya College …
80 PUBLICATIONS **407** CITATIONS
SEE PROFILE

Spectrochimica Acta Part A: Molecular and Biomolecular Spectroscopy 140 (2015) 44–53

Contents lists available at ScienceDirect

Spectrochimica Acta Part A: Molecular and Biomolecular Spectroscopy

journal homepage: www.elsevier.com/locate/saa

Investigation on growth, structure and characterization of succinate salt of 8-hydroxyquinoline: An organic NLO crystal

R. Thirumurugan [a], B. Babu [b], K. Anitha [a,*], J. Chandrasekaran [b]

[a] Department of Physics, School of Physics, Madurai Kamaraj University, Madurai 625021, Tamilnadu, India
[b] Department of Physics, Sri Ramakrishna Mission Vidyalaya College of Arts and Science, Coimbatore 641020, Tamilnadu, India

HIGHLIGHTS

- Grown crystal shows good optical transmittance in the entire visible region.
- Thermal studies gives, the compound is stable up to 145°C.
- Chemical structure of compound was established by NMR and IR technique.
- Powder SHG efficiency was 1.3 times greater than that of standard KDP.

GRAPHICAL ABSTRACT

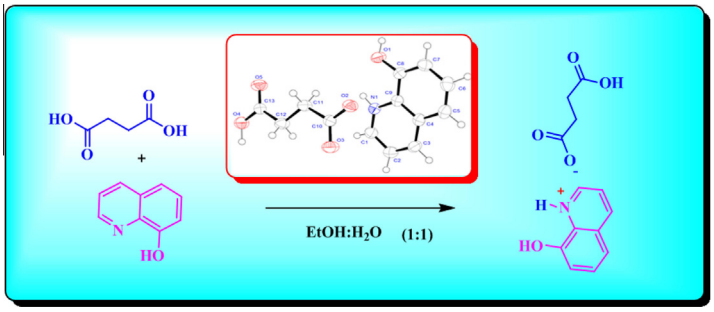

ARTICLE INFO

Article history:
Received 30 April 2014
Received in revised form 24 December 2014
Accepted 26 December 2014
Available online 2 January 2015

Keywords:
Crystal growth
Single crystal X-ray diffraction
Thermal analysis
Dielectric constant
Nonlinear optical materials

ABSTRACT

8-Hydroxyquinolinium succinate (8-HQSU) has been synthesized and single crystals were grown from ethanol solvent by employing the technique of slow evaporation at room temperature. The structure of the grown crystal has been elucidated by single crystal X-ray diffraction analysis. It reveals that 8-HQSU crystallizes in monoclinic system with non-centro symmetric space group $P2_1$. FTIR, ^1H and ^{13}C NMR spectral investigations have been carried out to identify the vibrational modes of various functional groups and placement of proton and carbon in the 8-HQSU compound, respectively. UV–vis–NIR transmission spectrum shows the cutoff wavelength around 357 nm. In addition, a photoluminescence spectral analysis was carried out for 8-HQSU crystals. The thermal properties of crystals were evaluated from TGA and DTA techniques and the crystal was found to be stable up to 145 °C. The dielectric studies show that the dielectric constant and dielectric loss decrease exponentially with frequency at different temperatures. Photoconductivity studies were carried out on the grown crystals it reveals the positive photo conducting nature. Powder second harmonic generation property of the crystal was confirmed by Kurtz and Perry powder SHG technique and it is found to be 1.3 times greater than that of KDP.

Introduction

Nonlinear optical materials play a pivotal role in the evolution of modern technology because its impact on technology and industrial applications in particular [1]. It exhibits a wide range of applications in optical information processing, telecommunication and integrated optics [2]. In the aspect of large second-order optical susceptibilities, ultrafast response time and high laser damage threshold to laser irradiation for opto-electronic applications such as high speed information processing, optical switching, electro-optic modulators, optical parametric oscillation, optical communications and optical data storage organic NLO materials have several advantages over inorganic counterparts [3–12]. Organic functionalized NLO materials attracted a great deal of attention

* Corresponding author. Tel.: +91 452 2458471 (308).
E-mail address: singlecrystalxrd@gmail.com (K. Anitha).

http://dx.doi.org/10.1016/j.saa.2014.12.093
1386-1425/

due to its extensive applications in harmonic generation, amplitude, phase modulation, switching and other signal processing devices [13–15]. These results show that crystals composed of organic molecules offer good perspectives for industrial applications and could represent an important advance in the search for compatible acentric crystal structures with good nonlinear responses. A possible reason for the significant increase in the effective nonlinear optical response observed in organic molecules is due to the existence of π-conjugation between the appropriate electron donor and acceptor groups, chirality and hydrogen bonding. In this communication we report the results of 8-hydroxyquinoline (8-HQ) a functional organic compound complexed with succinic acid for assembling second-order NLO material. Because 8-HQ is a quinoline based aromatic heterocyclic compound, which have enhanced non-centrosymmetry due their lack of inversion symmetry [16–18]. Also, this molecule has been complexed with a large number of organic and inorganic crystalline materials, some of them with outstanding physical properties, for example 8-HQ with aluminum complex is used as the organic white light emitting diode and 8-hydroxyquinolinium maleate exhibits second harmonic generation (SHG) efficiency 7 times greater than that of KDP [19,20]. While succinic acid is a diprotic, dicarboxylic acid, it forms crystalline succinates with organic molecules easily. A series of second-order NLO active materials composed of succinate have been synthesized, such as L-valinium succinate, L-prolinium succinate and L-alaninium succinate [21–23]. 8-HQSU is one such π donor–acceptor molecular compound in which 8-hydroxyquinoline acts as donor and succinic acid as electron acceptor. Previously synthesis, single crystal XRD lattice parameters, FTIR and optical transmittance (200–900 nm) studies were reported by the present authors [24]. In this present investigation, we report, full structural, spectral, optical (200–1100 nm), thermal, dielectric, photoconductivity, photoluminescence, microhardness and powder second harmonic generation (SHG) properties of 8-hydroxyquinolinium succinate (8-HQSU) single crystal.

Experimental procedure

Material synthesis and crystal growth method

The title compound was synthesized by dissolving equimolar ratio of commercially available AR grade 8-hydroxyquinoline (Merck) in ethanol solution and succinic acid (SRL) in the aqueous solution. The solution was prepared by continuous stirring for two hours at the room temperature and then filtered in a clean vessel. Then the prepared solution was covered by the perforated polythene paper to control the fast evaporation of the solvent and kept for slow evaporation. The crystalline substances were obtained from the solution within a week. The reaction mechanism of compound is shown in Fig. 1. The purity of the synthesized compound was improved by successive recrystallization process and filtration. The saturated solution of the crystallized salt was prepared using ethanol as solvent and kept for slow evaporation. Optically good quality yellow colored single crystals of 8-HQSU were harvested from the saturated solution within a week, which is suitable for single crystal X-ray diffraction analysis. The density of the grown crystal was determined as 1.47 (2) Mg m^{-3} by the flotation method using a liquid mixture of carbon tetrachloride (1.59 Mg m^{-3}) and xylene (0.89 Mg m^{-3}). The melting point of the grown crystal was measured as 145(2) °C. The photograph of as grown crystal is shown in Fig. 2a The growth morphology of 8-HQSU (Fig. 2b) has been deduced by the Bravais–Friedel Donnay–Harker (BFDH) model [25,26], where the CIF data obtained from the single crystal X-ray diffraction study were used as input and found that the depicted morphology of the crystal agree well with the morphology of the grown crystals.

Characterization

To confirm the chemical structure of 8-HQSU crystal, the ^{1}H and ^{13}C NMR spectra were recorded by employing a Bruker 500 MHz spectrometer in deuterated solvents using DMSO as the internal reference standard. X-ray data for the title compound were collected at room temperature using Enraf–Nonius CAD4 diffractometer with MoKα radiation, λ = 0.71073 Å, graphite monochromator. A suitable prismatic crystal was selected for X-ray diffraction and mounted on the goniometer. The position of the crystal was aligned perfectly. Lattice constants were obtained from a least-squares fit of 25 reflections within $9 < \theta < 11$. Within the collection limits (h 0 to 11, k – 1 to 5, l – 15 to 15) 1489 reflections were measured using $\omega/2\theta$ scan mode. Three check reflections monitored for every 2 h revealed no intensity decay. Cell refinement and data reduction were carried out using CAD-4 EXPRESS [27] and XCAD4 [28]. The intensities were corrected for Lorentz and polarization

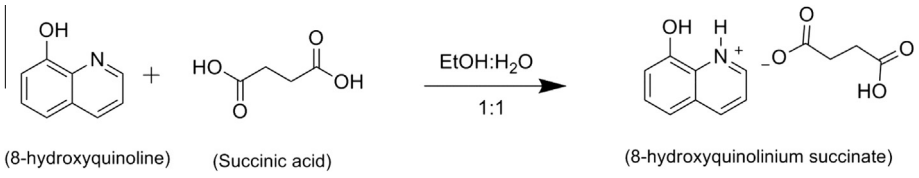

Fig. 1. Reaction scheme of 8-HQSU.

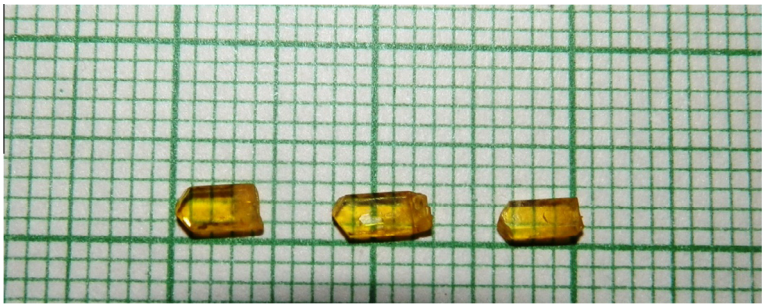

Fig. 2a. Photograph of as grown crystals of 8-HQSU.

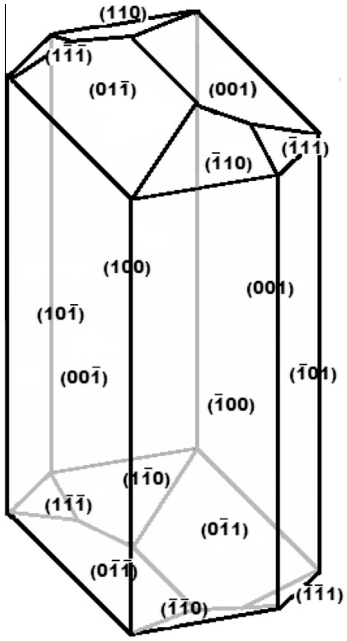

Fig. 2b. Morphology of the 8-HQSU single crystal.

Table 1
Crystal data and structure refinement for 8-HQSU crystal.

Empirical formula	C_{13} H_{13} N O_5
Formula weight	263.24
Temperature	293(2) K
Wavelength	0.71073 Å
Crystal system, space group	Monoclinic, $P2_1$
Unit cell dimensions	a = 9.549(1) Å
	b = 4.974(5) Å β = 104.04(5)°
	c = 12.678(8) Å
Volume	584.2(7) Å^3
Z, calculated density	2, 1.497 Mg/m^3
Absorption coefficient	0.116 mm^{-1}
F(000)	276
θ range for data collection	2.20–24.98 °
Limiting indices	$0 \leqslant h \leqslant 11$, $-1 \leqslant k \leqslant 5$, $-15 \leqslant l \leqslant 15$
Reflections collected/unique	1489/1406 [R (int) = 0.0167]
Completeness to θ = 24.98°	99.3%
Refinement method	Full-matrix least-squares on F^2
Data/restraints/parameters	1406/1/174
Goodness-of-fit on F^2	1.191
Final R indices [$I > 2\sigma$ (I)]	R1 = 0.0321, wR2 = 0.0899
R indices (all data)	R1 = 0.0326, wR2 = 0.0905
Largest diff. peak and hole	0.173 and −0.138 e Å^{-3}
CCDC NO	943652

Table 2
Selected bond lengths (Å) and bond angles (°) for 8-HQSU crystal.

Atoms	Lengths (Å)	Atoms	Angles (°)
O(5)—C(13)	1.324(3)	C(8)—N(1)—C(7)	122.3(2)
O(2)—C(10)	1.247(3)	N(1)—C(7)—C(2)	119.45(18)
O(3)—C(10)	1.257(3)	N(1)—C(7)—C(6)	120.0(2)
O(1)—C(6)	1.344(3)	C(2)—C(7)—C(6)	120.5(2)
O(4)—C(13)	1.200(3)	C(3)—C(2)—C(1)	122.8(2)
N(1)—C(8)	1.320(3)	C(3)—C(2)—C(7)	119.4(2)
N(1)—C(7)	1.365(3)	C(1)—C(2)—C(7)	117.7(2)
C(7)—C(2)	1.414(3)	O(1)—C(6)—C(5)	125.75(19)
C(7)—C(6)	1.420(3)	O(1)—C(6)—C(7)	116.41(19)
C(2)—C(3)	1.404(4)	C(5)—C(6)—C(7)	117.8(2)
C(2)—C(1)	1.414(3)	C(6)—C(5)—C(4)	121.7(2)
C(6)—C(5)	1.361(3)	C(13)—C(12)—C(11)	114.19(18)
C(5)—C(4)	1.404(4)	O(2)—C(10)—O(3)	122.9(2)
C(12)—C(13)	1.504(3)	O(2)—C(10)—C(11)	119.82(19)
C(12)—C(11)	505(3)	O(3)—C(10)—C(11)	117.28(18)
C(10)—C(11)	1.518(3)	C(9)—C(1)—C(2)	120.2(2)
C(1)—C(9)	1.364(4)	C(1)—C(9)—C(8)	119.7(2)
C(9)—C(8)	1.396(4)	O(4)—C(13)—O(5)	119.3(2)
C(3)—C(4)	1.359(3)	O(4)—C(13)—C(12)	123.9(2)
O(5)—C(13)—C(12)	116.80(18)	C(12)—C(11)—C(10)	115.16(18)
C(4)—C(3)—C(2)	119.1(2)	C(3)—C(4)—C(5)	121.4(2)
N(1)—C(8)—C(9)	120.6(2)		

Table 3
Selected torsion angles (°) for 8-HQSU crystal.

Atoms	Angles (°)	Atoms	Angles (°)
C(8)—N(1)—C(7)—C(2)	0.8(3)	C(11)—C(12)—C(13)—O(5)	178.9(2)
C(8)—N(1)—C(7)—C(6)	−178.4(2)	C(1)—C(2)—C(3)—C(4)	−179.9(2)
N(1)—C(7)—C(2)—C(3)	−179.3(2)	C(7)—C(2)—C(3)—C(4)	−0.8(4)
C(6)—C(7)—C(2)—C(3)	−0.1(3)	C(13)—C(12)—C(11)—C(10)	−178.6(2)
N(1)—C(7)—C(2)—C	−0.2(3)	O(2)—C(10)—C(11)—C(12)	2.8(3)
C(6)—C(7)—C(2)—C(1)	179.0(2)	O(3)—C(10)—C(11)—C(12)	−177.7(2)
N(1)—C(7)—C(6)—O(1)	0.8(3)	C(2)—C(3)—C(4)—C(5)	0.7(4)
C(2)—C(7)—C(6)—O(1)	−178.4(2)	C(6)—C(5)—C(4)—C(3)	0.3(4)
N(1)—C(7)—C(6)—C(5)	−179.7(2)	C(7)—N(1)—C(8)—C(9)	−0.6(4)
C(2)—C(7)—C(6)—C(5)	1.1(3)	C(1)—C(9)—C(8)—N(1)	−0.1(4)
O(1)—C(6)—C(5)—C(4)	178.3(2)	C(11)—C(12)—C(13)	−0.9(4)
C(7)—C(6)—C(5)—C(4)	−1.2(4)	C(2)—C(1)—C(9)—C(8)	0.7(4)
C(3)—C(2)—C(1)—C(9)	178.6(3)	C(7)—C(2)—C(1)—C(9)	−0.6(4)

Table 4
Selected hydrogen bond geometry (Å, °) for 8-HQSU crystal.

D—H···A	d (D—H) (Å)	d (H···A) (Å)	d (D···A) (Å)	<(DHA) (°)
O1—H7···O2 i	0.886(5)	1.839(1)	2.712(2)	168.15(3)
N1—H8···O2 ii	0.929(2)	1.838(5)	2.732(7)	160.57(1)
O4—H13···O3 ii	0.985(4)	1.607(6)	2.590(2)	175.76(2)

Symmetry codes: (i) $-x$, $y-1/2$, $-z$, (ii) x, $y-1$, z, (iii) $-x$, $y-1/2$, $-z+1$.

effects. The structure was solved by direct methods as implemented in SHELXS-97 [29] program. The position of all the non-hydrogen atoms were included in the full-matrix least squares refinement using SHELXL-97 [29] program. The molecular graphics were depicted by the program ORTEP-3 for windows [30] and MERCURY (version 1.4.1) [31]. All the hydrogen atoms were placed in geometrically calculated positions and included in the refinement in the riding model approximation with Uiso(H) equal to 1.2 Ueq of the carrier atom. The crystal data and details pertaining to data collection and the structure refinement are given in Table 1. Selected bond lengths, bond angles and torsion angles are given in Tables 2 and 3, respectively. The hydrogen bond data are given in Table 4. Fig. 3a shows the ORTEP view of the molecule drawn at 50% probability thermal displacement ellipsoids with the atom numbering scheme. Fig. 3b shows crystal packing diagram of the 8-HQSU molecule. Powder XRD measurements were also carried out by using PANalytical XPERT-PRO powder X-ray diffractometer with nickel filtered, CuKα radiation of wavelength 1.5418 Å the 2θ range between 5 and 80° by employing the reflection mode for scanning with a scan speed of 1 s and step size of 0.02°. The indexed powder X-ray diffraction (PXRD) pattern of 8-HQSU is shown in Fig. 1s and obtained lattice parameters were compared with single crystal X-rd data and is given in Table 1s (Refer Supplementary material). The FTIR spectrum of 8-HQSU was recorded using JASCO FT/IR-410 spectrometer using KBr pellet technique in the range 4000–400 cm^{-1} at room temperature. The UV–vis–NIR transmission spectrum of 8-HQSU crystal was recorded with Shimadzu UV2450 spectrophotometer in the range of 200–1100 nm with photomultiplier tube. The photoluminescence spectra of the crystals have been recorded using the Shimadzu RF5301 spectroflourometer with 450 W high pressure Xenon lamp as excitation source at room temperature. Single crystals of 8-HQSU were

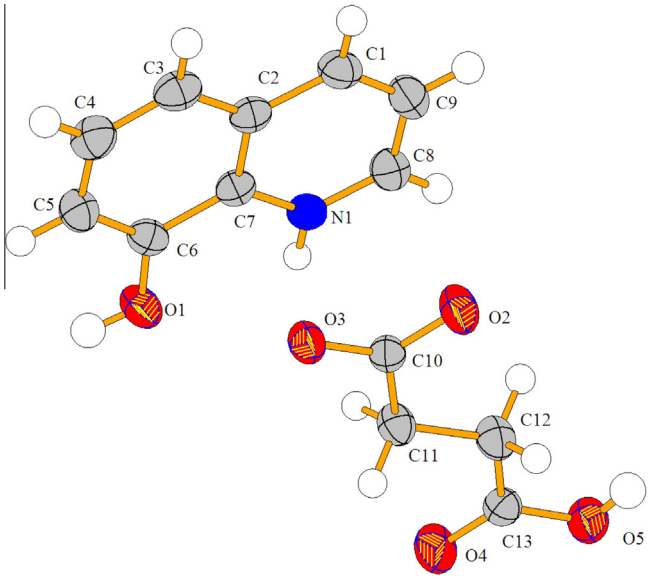

Fig. 3a. ORTEP diagram of the 8-HQSU crystal.

subjected to thermo gravimetric analysis (TGA) and differential thermal analysis (DTA) simultaneously in nitrogen atmosphere at a heating rate of 10 K/min using NETZSCH STA 409 °C/CD instrument. Dielectric studies for the grown crystals were carried out using Hioki LCR 3532-50 LCR meter. All the measurements were carried out in the frequency range from 50 Hz to 5 MHz at different temperature. Photoconductivity studies for the grown crystals were carried out using Keithley 6517B electrometer. Microhardness studies for the grown 8-HQSU crystals were carried out using a Shimadzu HMV-2000 Vickers Microhardness pyramidal indenter. A Q-switched Nd:YAG laser beam of the wavelength of 1064 nm was used for SHG measurements with an input power of 3.4 mJ/pulse.

Results and discussions

NMR spectral studies

In ^{1}H NMR the appearance of doublet of doublet at δ 8.80 ppm clearly indicates the C2 (imine CH) proton of the quinoline moiety. The appearance of doublet of doublet in the region δ 8.18 ppm indicates the proton attached in C4 position of quinoline moiety. The multiplet (two doublets) appeared in δ 7.41–7.48 ppm is due to C5 and C6 protons. The appearance of multiplet at δ 7.32–7.35 is due to the C3 proton. The appearance of multiplet at δ 7.14–7.17 ppm is due to C7 proton. The N^+H proton and the OH protons of 8-hydroxyquinolinium moiety in the complex are far down field shifted and do not appear in the spectrum at all. The ^{1}H NMR spectra of the 8-HQSU crystal is depicted in Fig. 4a. In ^{13}C NMR the peak at δ 173.74 clearly indicates the presence of carbonyl carbon. The peak appeared in δ 153.57 clearly indicates the presence of iminium carbon. The peak appeared at δ 28.89 is due to the presence of succinate alkyl carbon. The ^{13}C NMR spectrum of the 8-HQSU crystal is depicted in Fig. 4b. On the basis of the above chemical shift values the molecular structure of the 8-hydroxyquinolinium succinate salt is confirmed.

Single crystal X-ray diffraction studies

The crystal formed by 8-hydroxyquinoline with succinic acid is a salt, namely 8-hydroxyquinolinium succinate, $C_9H_8N_1O_1^+.C_4H_5O_4^-$. The protonation occurred at the endocyclic N-site of the 8-hydroxyquinoline leading to the formation of cation is confirmed by the enhancement of the internal angle at N1, in the 8-Hydroxyquinolinium cation (C9—N1—C1 bond angle of 122.12(2)°) compared with 119.03° observed in neutral 8-hydroxyquinoline moiety [32]. The other bond distances and bond angles of cation are comparable with those found in the maleate and fumarate salts of 8-hydroxyquinoline cations [33]. The deprotonation occurred at one of the carboxylic acids of succinic acid molecule, leading to an anion (Fig. 3a) which can be corroborated by the variations of the carboxyl C—O, C═O and C⎓O bond distances (d (C10⎓O2) = 1.249(6) Å, d (C10⎓O3) = 1.255(6) Å). The 8-hydroxyquinolinium cation and succinate anion are essentially planar, with maximum deviations of 0.011 (1) Å and 0.020 (1) Å, respectively. The dihedral angle between these two planes is 11.02 (6)°, indicating they are approximately parallel to each other. Due to the existence of complementary functional groups, extensive hydrogen bonds form easily. The cation is linked to anion through an ionic N^+—H···O^- (x, $y-1$, z) and O—H···O intermolecular hydrogen bonds that produce $R_4^2(14)$ motif. The crystal structure of 8-HQSU is thus stabilized by a network of N—H···O and O—H···O hydrogen bonds.

FTIR spectral studies

The FTIR spectrum of 8-HQSU crystal is depicted in Fig. 5. The O—H stretching vibration appears at 3400 cm^{-1}. The Aromatic

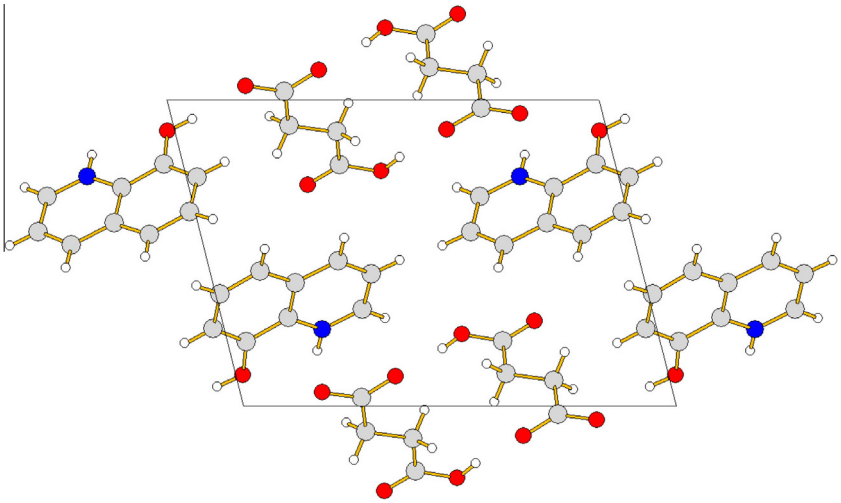

Fig. 3b. Crystal packing diagram of 8-HQSU.

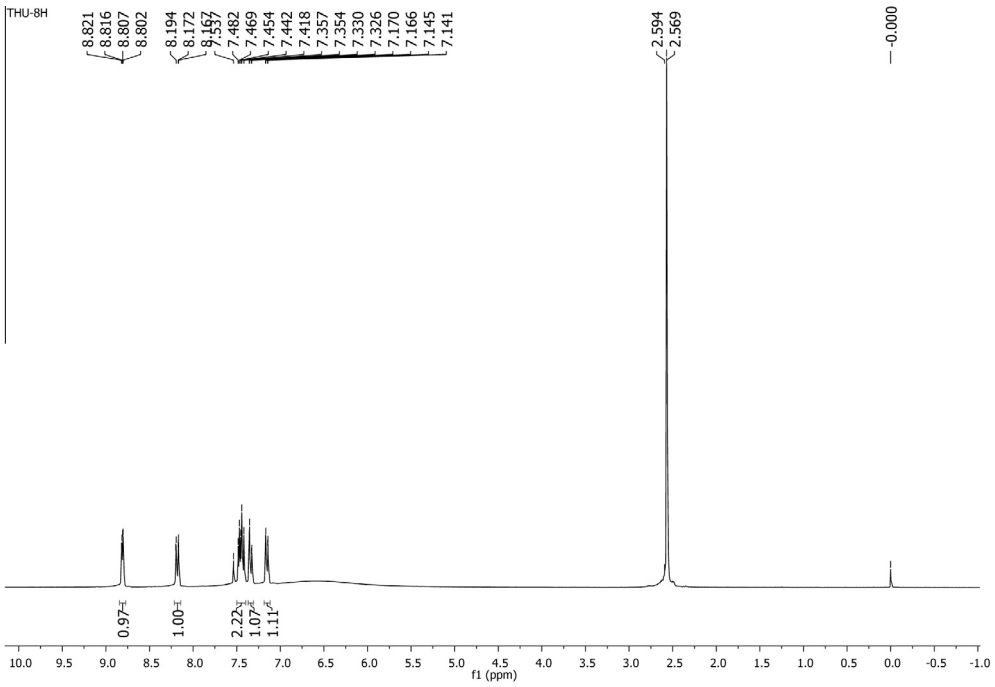

Fig. 4a. ^{1}H NMR spectrum of the 8-HQSU crystal.

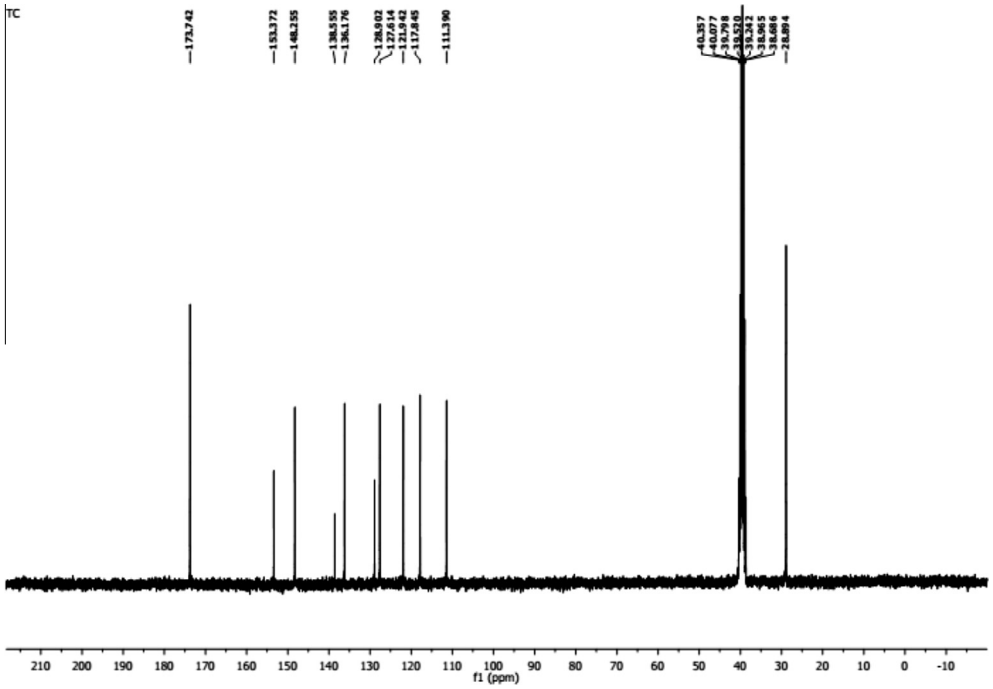

Fig. 4b. ^{13}C NMR spectrum of the 8-HQSU crystal.

C—H stretching appears at 3059 cm^{-1}. The absorption band at 2928 cm^{-1} can be assigned as symmetric C—H stretching vibrations of —CH_2 groups. The peak observed at 1602 cm^{-1} is assigned to C=N ring stretching vibration. The peak ascribed at 1416 cm^{-1} is due to the C—O—H plane bending vibration. The band near 700 cm^{-1} represents the C—OH stretching [34]. The carbonyl stretching vibrations band at 1742 cm^{-1} as well as anti-symmetric and symmetric stretching vibration bands (1543 and 1375 cm^{-1}) of COO^{-} group are obtained [35]. The peak at 939 cm^{-1} is attributed to symmetric C—C stretching, respectively [36]. The band observed at 875 cm^{-1} is assigned to out of plane bending of C—O deformation [37]. The observed peak at 1030 cm^{-1} is assigned to ring breathing mode and which is in good agreement with the breathing modes of quinoline and isoquinoline. Also the vibrations around 750–500 cm^{-1} are assigned to in-plane bending vibration of quinoline [16]. The C—C in plane and out plane bending vibrations were observed at 1030 and 802 cm^{-1}.

UV–vis–NIR spectral studies

The recorded UV–vis–NIR transition spectrum is shown in Fig. 6. Optical transmission range and the cutoff wavelength of

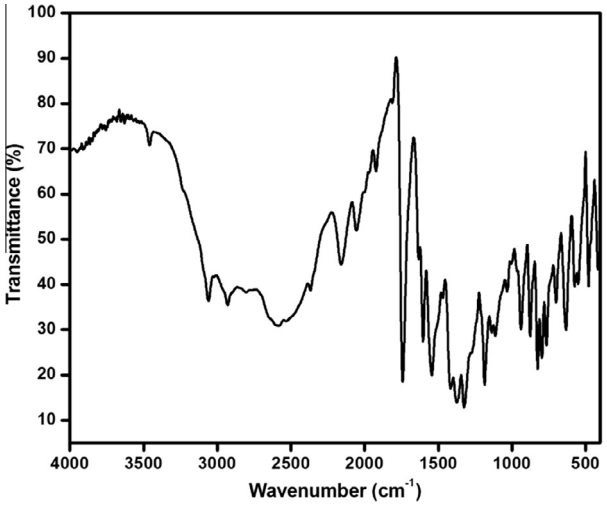

Fig. 5. FT-IR Spectrum of 8-HQSU crystal.

single crystals are very important factor for optical applications. The cut-off wavelength of the 8-HQSU is observed at 357 nm, and the crystal shows good transmittance percentage in the range of 357–1100 nm. From the recorded spectrum, it is observed that the crystal has high transmittance of above 80% in the entire visible region. This property attests the suitability of the crystal good for various optoelectronic applications [38].

Determination of optical constant

The optical absorption coefficient (α) calculated from the measured transmittance (T) values by the following relation.

$$\alpha = -\frac{1}{t}\ln\left(\frac{1}{T}\right)$$

where t is the thickness of the sample. The optical bandgap (E_g) is evaluated from the optical absorption coefficient near the absorption edge is given by

$$\alpha = \frac{A(h\nu - E_g)^2}{h\nu}$$

where, A is a proportional constant, h is the planks constant, E_g is the optical band gap of the crystal and ν is the frequency of the incident photons. E_g was evaluated by extrapolation of the linear part (Fig. 7). The estimated band gap is about 3.45 eV. This is comparatively higher than the 8-hydroxyquinolinium hydrogen maleate [20]. Crystals with higher band gap expected to possess large transmittance in the visible region [39]. The optical constants such as refractive index (n) and extinction coefficient (K) are determined from the transmission (T) and reflectance (R) spectrum based on the following relations

$$T = \frac{(1-R)^2\exp(-\alpha t)}{1-R^2\exp(-2\alpha t)}$$

where t is the thickness and α is related to extinction coefficient by $K = \frac{\alpha\lambda}{4\pi}$

The reflectance (R) in terms of the absorption coefficient and refractive index (n) can be derived from the relations:

$$R = \frac{1 \pm \sqrt{(1-\exp(-\alpha t)+\exp(\alpha t))}}{1+\exp(-\alpha t)}$$

$$n = \frac{-(R+1) \pm \sqrt{(-3R^2+10R-3)}}{2(R-1)}$$

Fig. 8 shows the variation of refractive index (n) as a function of wavelength. Hence, by tailoring the absorption coefficient, one can get the desired material to fabricate the optoelectronic devices. The refractive index decreases with increase in wavelength. The refractive index (n) is 1.8 at 600 nm for 8-HQSU crystal.

Photoluminescence studies

The sample was excited at 357 nm and the emission spectrum was measured in the range 375–600 nm. The recorded emission spectrum is depicted in Fig. 9. The maximum emission peak was observed to be at 421 nm. In the conversion from wavelength to energy, the energy band gap at this wavelength was calculated to be 2.95 eV using the formula $E_g = hc/\lambda e$. Where h, c, e is constants and λ is the wavelength of fluorescence. The results indicate that the 8-HQSU single crystal has a violet emission; it suggests that it can be used as a new violet-light emitting material.

Thermal studies

From the Fig. 10, the DGA curve shows a sharp endothermic peak at 145 °C. The sharpness of the endothermic peak at 145 °C shows the melting point of the 8-HQSU crystal and good crystalline

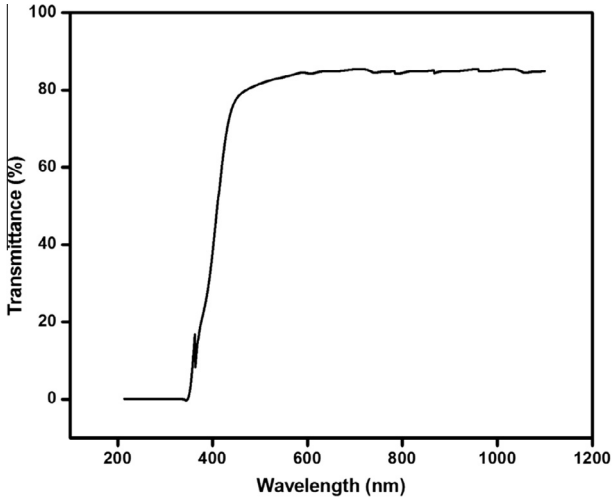

Fig. 6. UV–vis spectrum of 8-HQSU crystal.

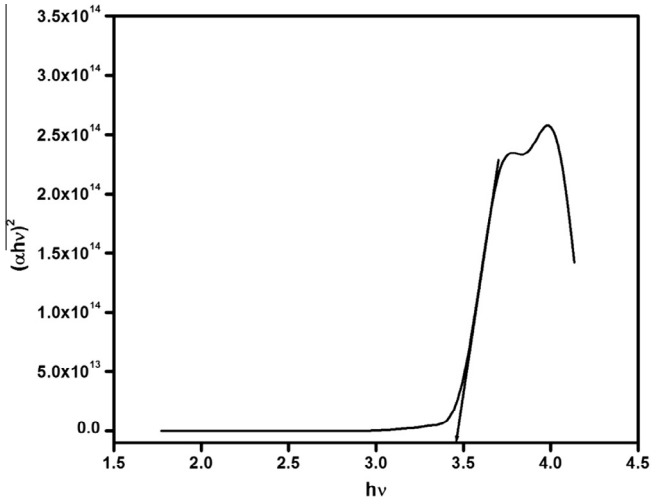

Fig. 7. Optical band gap spectrum of 8-HQSU.

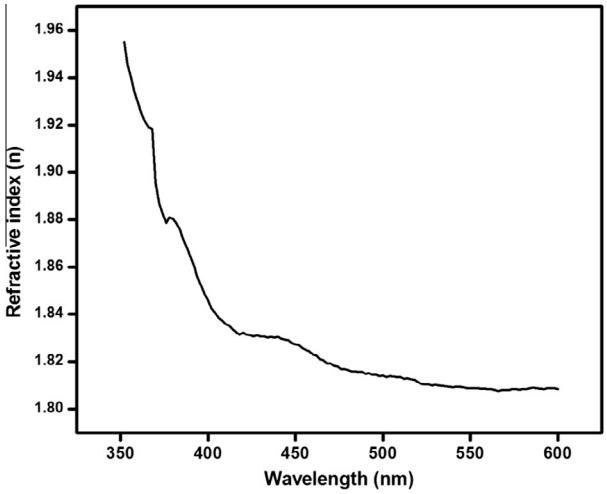

Fig. 8. Refractive index of 8-HQSU.

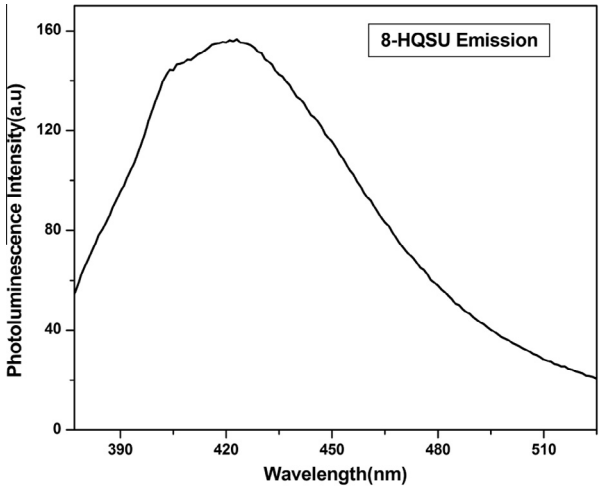

Fig. 9. Luminescence emission spectrum of 8-HQSU crystal.

perfection of the synthesized compound. TGA curve of the sample shows that material is highly stable up to 130 °C, and there is no phase transition up to 130 °C, and it is also indicating that the absence of the water molecule in the material. The major weight loss of about 78.6% in the temperature range 145–200 °C after that the remaining 12.4% molecules decomposed. Peaks above 300 °C are due to the liberation of volatile substances and gases such as CO, CO_2, and NH_3 [11]. From the TG/DTA results it can be concluded that the grown 8-HQSU crystal can be utilized for optoelectronic device applications up to 130 °C.

Dielectric studies

Dielectric properties are correlated with the lattice dynamics in the crystal. Also it provides useful information such as nature of atoms, defects, ions and their bonding as well as polarization mechanism in the materials. The measurement of dielectric constant and dielectric loss has been done as a function of different frequencies at different temperature and are shown in Figs. 11 and 12. The dielectric constant of the crystal can be calculated using the following relation

$$\varepsilon_r = \frac{Cd}{\varepsilon_0 A}$$

where C is the capacitance and d is the thickness, A is the cross sectional area of the sample and ε_o is the free space permitivity of the sample. From the Fig. 11, the value of dielectric constant decreases with increase in frequency for all the temperatures and remains constant at higher frequencies. The high value of dielectric constant of 8-HQSU crystal at low frequencies may be attributed to the contribution of polarizations, namely space charge, orientational, electronic and ionic polarizations and its low value at higher frequencies may be due to the loss of significance of these polarizations gradually [40]. In accordance with Miller rule, the lower value of dielectric constant at higher frequencies is a suitable parameter for the enhancement of second harmonic generation coefficient [41]. From Fig. 12, the characteristic of low dielectric loss with high frequency for the sample suggests that the crystal possess enhanced optical quality with fewer defects which is the desirable property for NLO applications.

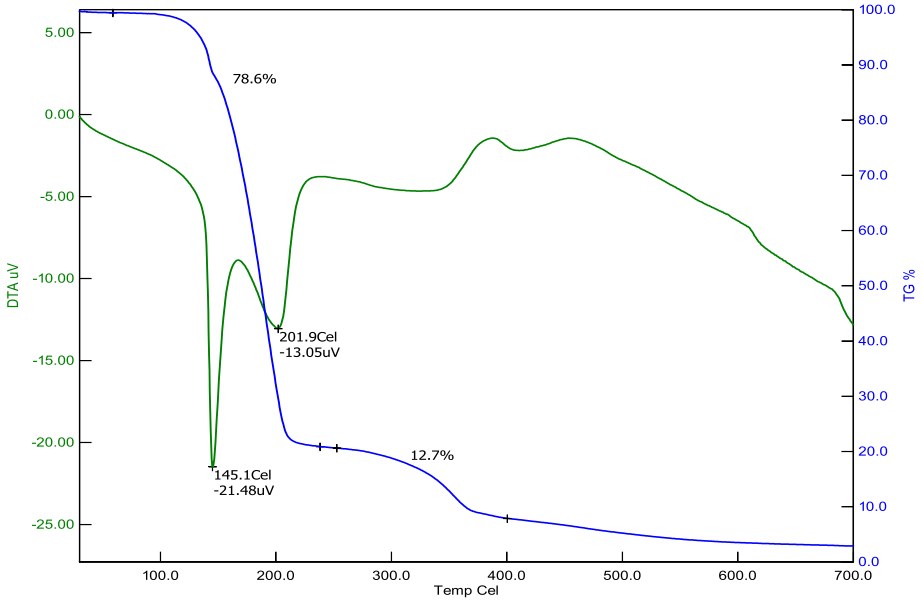

Fig. 10. TGA/DTA curve of 8-HQSU crystal.

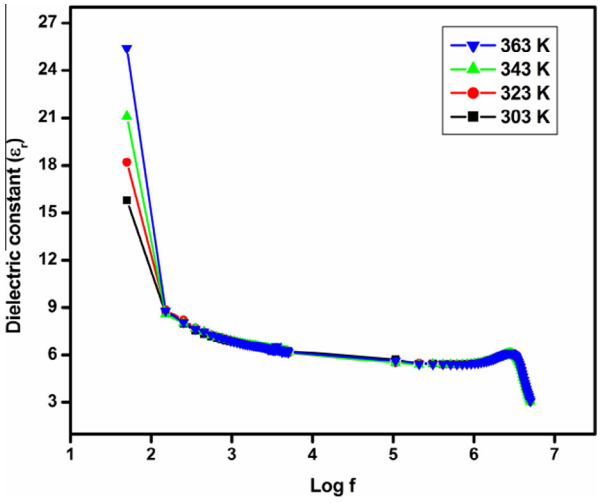

Fig. 11. Variation of dielectric constant with log frequency at different temperatures for 8-HQSU single crystal.

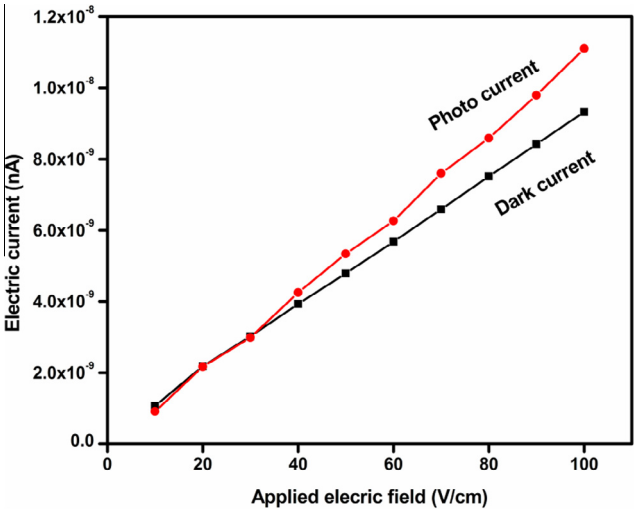

Fig. 13. Field dependent photoconductivity of 8-HQSU single crystal.

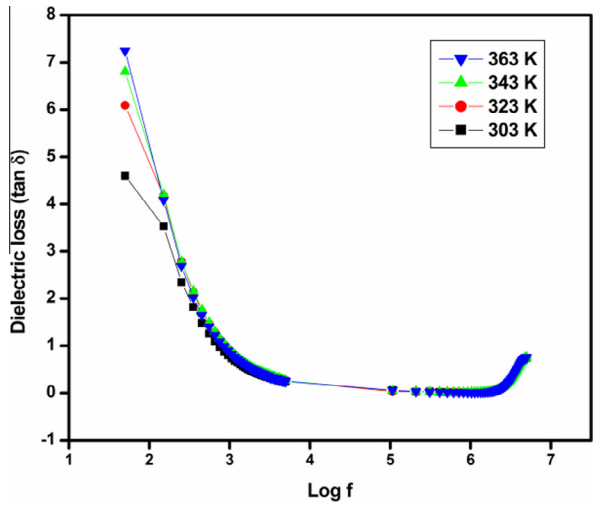

Fig. 12. Variation of dielectric loss with log frequency at different temperatures for 8-HQSU single crystal.

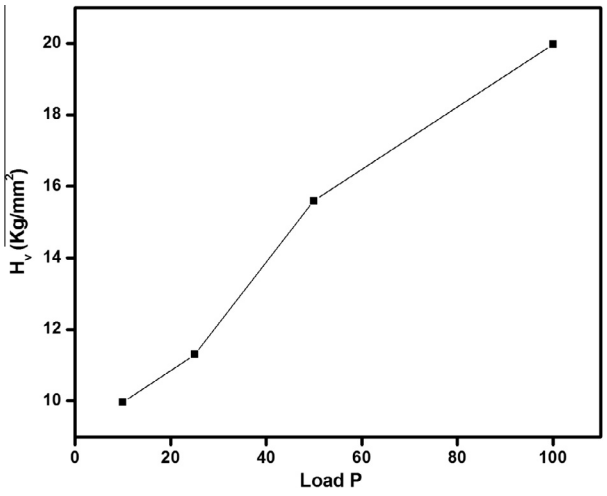

Fig. 14. Hardness vs Applied load.

Photoconductivity studies

In order to get ohmic contact, opposite faces of polished crystal were painted using electronic grade silver paste and two thin copper wires were connected on the both sides of the sample. Then the samples were connected in series with DC power supply. Photocurrent and dark current were recorded as function of input applied voltage. All the measurements were recorded at room temperature. The input voltage was increased from 10 V to 100 V. The sample was prevented from all the radiations and resultant dark current was recorded. In order to obtain photocurrent, sample was exposed to the radiation from 100 W halogen lamp containing iodine vapor and tungsten filaments. Corresponding photocurrent was recorded for the same applied electric field. Fig. 13 shows the variation of both dark current (I_d) and photocurrent (I_p) with applied field. It is seen from the plots that both I_p and I_d of the samples were increases linearly with applied electric field. It is interesting to note that the photo current is always higher than the dark current, which is termed as positive photo conductivity. This may be attributed to large number of mobile charge carriers generated by absorption of photons [42].

Mechanical studies

Microhardness of the material is one of the important mechanical properties of the material. Also it plays a vital role in the device fabrication. Microhardness test is a microprobe technique for evaluating the bond strength, apart from being a measure of bulk strength [43]. Transparent polished crystals with smooth surfaces (crack free) were selected for the microhardness measurements. All the indentations were made at room temperature by using a Shimadzu HMV-2000 fitted with the Vickers diamond pyramidal indenter. The applied load P is varied between 10 and 100 g, and all the indentation time was kept as 9 s for all the loads. Several indentations were made for each load and the average value of the diagonal length was used to calculate the Vickers microhardness number. The Vickers microhardness number was calculated using the given expression

$$H_v = 1.8554\left(\frac{P}{d^2}\right)(\mathrm{kg/mm})^2$$

where P is the applied load in g, d is the diagonal length of the indented impression (μm) and 1.8554 is a constant of a geometrical factor for the diamond pyramid. Fig. 14 shows the Vickers

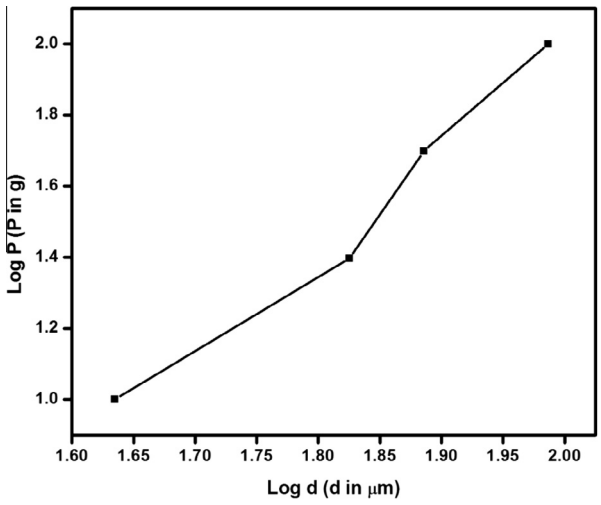

Fig. 15. Log *P* vs Log *d*.

Table 5
Powder SHG comparison of 8-HQSU.

Compound name	Powder SHG efficiency	References
8-Hydroxyquinolinium hydrogen maleate	7 times of KDP	[20]
L-Valinium succinate	0.56 times of KDP	[21]
L-Alanium succinate	0.77 times of KDP	[23]
8-Hydroxyquinolinium succinate	1.3 times of KDP	Present work

microhardness number with applied load for 8-HQSU crystal. For load above 100 g micro cracks were developed around the indentation mark. It may be due to the release of internal stress generated locally by indentation. The increase of hardness attributed to the work hardening of the surface layers and it exhibits the reverse indentation size effect (RISE). Fig. 15 depicts the Log*P* against Log*d* and it gives the value of '*n*', which is determined to be 2.8. According to Onitsch [44] and Hanneman [45] '*n*' should lie between 1 and 1.6 for harder materials and above 1.6 for softer materials. Hence the grown 8-HQSU crystal belongs to the soft material category.

SHG studies

The most widely used technique for confirming the SHG efficiency of NLO materials is Kurtz–Perry powder SHG method [46]. A Q-switched Nd:YAG laser beam of wavelength of 1064 nm with an input power of 3.4 mJ and pulse width of 8 ns with a repetition rate of 10 Hz was used. Grown 8-HQSU crystals were powdered with a uniform particle size of 125–150 μm, and then packed in a microcapillary of uniform bore and exposed to laser radiation. Microcrystalline KDP (Potassium dihydrogen phosphate) of the same particle size was used as reference material. The emission of green radiation from the sample confirms the second harmonic generation property. This green output is finally detected by a photomultiplier tube (Hamamatsu R5109) and displayed on a storage oscilloscope (TDS 3052 B 500 MHz, Phosphor digital oscilloscope). The obtained SHG signal outputs are 9 mV and 11.6 mV for KDP and 8-HQSU, respectively. The SHG efficiency of the title compound is found to be 1.3 times greater than that of KDP. Powder SHG efficiency of 8-HQSU is compared with some of the 8-hydroxyquinilinium and succinic acid organic crystals and given in Table 5.

Conclusion

Organic single crystals of 8-HQSU were grown from ethanol solvent by slow evaporation solution technique. The structure of grown crystal is ascertained by X-ray diffraction analysis and it is found that the crystal belongs to monoclinic system with space group $P2_1$. Chemical constructions and vibrational modes of various functional groups present in the crystal have been confirmed by ^{1}H, ^{13}C NMR and FT-IR spectroscopic analysis. The lower cutoff wavelength and transmission from entire visible region was determined from the UV–vis–NIR transmission spectrum. Photoluminescence property shows that the grown crystal is suitable for photonic device and laser-related applications. The result of TGA and DTA analysis pointed out the melting point of the crystal is around 145 °C. The sharp endothermic peak indicates the high quality of the crystal as well as its perfection. The dielectric studies reveal the low dielectric constant and dielectric loss of the crystal at high frequency region. The photoconductivity study ascertains the positive photoconducting nature of the 8-HQSU crystal. Vickers microhardness studies depicts that grown 8-HQSU belongs to soft material category. NLO studies confirm that the SHG efficiency of 8-HQSU is 1.3 times as large as that of the standard KDP crystal. The promising crystal growth characteristics and properties of 8-HQSU crystal indicate that it may be a potential material for photonic, electro-optic and SHG device application.

Acknowledgements

The authors thank the Department of Science and Technology (DST), India and University Grant Commission (UGC), India for establishing single crystal X-ray diffractometer, powder X-ray diffractometer and Vickers microhardness tester facilities at School of Physics, Madurai Kamaraj University, Madurai through DST-FIST, UGC-COSIST programmes.

Appendix A. Supplementary data

Supplementary data associated with this article can be found, in the online version, at http://dx.doi.org/10.1016/j.saa.2014.12.093.

References

[1] P.N. Prasad, D.J. Williams, Introduction to Nonlinear Optical Effect in Molecules and Polymers, John Wiley & Sons Inc, 1991.
[2] C. Bosshard, K. Sutter, P. Pretre, J. Hulliger, M. Flörsheimer, P. Kaatz, P. Günter, Organic Nonlinear Optical Materials, Gordon and Breach, Basel, 1995.
[3] S. Basu, Ind. Eng. Chem. Prod. Res. Dev. 23 (1984) 183.
[4] P.N. Prasad, D.R. Ulrich, Non-linear Optical and Electro Active Polymers, Plenum, New York, 1988.
[5] D.R. Kanis, M. Ratner, T.J. Marks, Chem. Rev. 94 (1994) 195.
[6] P. Pandi, G. Peramaiyan, M. Krishna Kumar, R. Mohan Kumar, R. Jayavel, Spectrochim. Acta A Mol. Biomol. Spectrosc. 88 (2012) 77.
[7] G. Peramaiyan, P. Pandi, B.M. Sornamurthy, G. Bhagavannarayana, R. Mohan Kumar, Spectrochim. Acta A Mol. Biomol. Spectrosc. 95 (2012) 310.
[8] N. Sudharsana, G. Subramanian, V. Krishnakumar, R. Nagalakshmi, Spectrochim. Acta A Mol. Biomol. Spectrosc. 97 (2012) 798.
[9] M. Shkir, H. Abbas, Spectrochim. Acta A Mol. Biomol. Spectrosc. 125 (2014) 453.
[10] M. Shkir, H. Abbas, Spectrochim. Acta A Mol. Biomol. Spectrosc. 118 (2014) 172.
[11] G. Bhagavannarayana, B. Riscob, Mohd. Shakir, Mater. Chem. Phys. 126 (2011) 20.
[12] I.P. Bincy, R. Gopalakrishnan, J. Cryst. Growth 402 (2014) 22.
[13] E.W. Van Stryland, H. Vanherzeele, M.A. Woodall, M.J. Soileau, A.L. Smirl, S. Guha, T.F. Bogess, Opt. Eng. 24 (1985) 613.
[14] T. Wei, D.J. Hagan, E.W. Van Stryland, IEEE 26 (1990) 760.
[15] J.J. Rodrigues Jr., L. Misoguti, F.D.C.R. Nunes Mendonca, S.C. Zilio, Opt. Mater. 22 (2003) 235.
[16] V. Krishnakumar, R. Nagalakshmi, P. Janaki, Spectrochim. Acta A Mol. Biomol. Spectrosc. 61 (2005) 1097.
[17] M. Rajasekaran, P. Anbusrinivasan, S.C. Mojumdar, J. Therm. Anal. Calorim. 100 (2010) 827.

[18] S.P. Prabhakaran, R. Ramesh Babu, P. Velusamy, K. Ramamurthi, Mater. Res. Bull. 46 (2011) 1781.
[19] C. Perez-Bolivar, S. Takizawa, G. Nishimura, V.A. Montes, P. Anzenbacher Jr., Chem. Eur. J. 17 (2011) 9076.
[20] G. Peramaiyan, P. Pandi, N. Vijayan, G. Bhagavannarayana, R. Mohan Kumar, J. Cryst. Growth 375 (2013) 6.
[21] C. Ramachandra Raja, A. Antony Joseph, Spectrochim. Acta A 74 (2009) 825.
[22] P. Balamurugaraj, S. Suresh, P. Koteeswari, P. Mani, J. Mater. Phys. Chem. 1 (2013) 4.
[23] C. Ramachandra Raja, G. Gokila, A. Antony Joseph, Spectrochim. Acta A Mol. Biomol. Spectrosc. 72 (2009) 753.
[24] R. Thirumurugan, K. Anitha, AIP Conf. Proc. 1591 (2014) 1226.
[25] E. Bravais, Crystallographiques, Academie des Sciences, Paris, 1913.
[26] J.D.H. Donnay, D. Harker, Am. Mineral. 22 (1937) 463.
[27] Enraf-Nonius, CAD-4 EXPRESS Version 5.1/1.2., Enraf–Nonius, Delft, The Netherlands, 1994.
[28] A.C.T. North, D.C. Phillips, F.S. Mathews, Acta Cryst. Sect. A 24 (1968) 351.
[29] G.M. Sheldrick, SHELXL97 and SHELXS97, University of Gottingen, Germany, 1997.
[30] L.J. Farrugia, J. Appl. Cryst. B 30 (1997) 565.
[31] C.F. Macrae, P.R. Edington, P. McCabe, E. Pidcock, G.P. Shields, R. Taylor, M. Towler, J. Van de Streek, J. Appl. Cryst. 39 (2006) 453.
[32] P. Roychowdhury, B.N. Das, B.S. Basak, Acta Cryst. B 34 (1978) 1047.
[33] S. Franklin, T. Balasubramanian, Acta Cryst. C 65 (2009) o58.
[34] K. Aravinth, G. Anandha Babu, P. Ramasamy, J. Therm. Anal. Calorim. 110 (2012) 1333.
[35] C. Ramachandra Raja, A. Antony Joseph, Spectrochim. Acta A Mol. Biomol. Spectrosc. 74 (2009) 825.
[36] S. Krishnan, C. Justin Raj, R. Robert, A. Ramanand, S. Jerome Das, Cryst. Res. Technol. 42 (2007) 1087.
[37] V.S. Dhanya, M.R. Sudarsanakumaran, S. Suma, S. Prasanna, K. Rajendra Babu, B. Suresh Kumar, S.M. Roy, J. Cryst. Growth 319 (2011) 96.
[38] D. Jaikumar, S. Kalainathan, G. Bhagavannarayana, Physica B 405 (2010) 2394.
[39] G. Shanmugam, K. Ravi Kumar, B. Sridhar, S. Brahadeeswaran, Mater. Res. Bull. 47 (2012) 2315.
[40] M. Vimalan, T. Rajesh Kumar, S. Tamilselvan, P. Sagayaraj, C.K. Mahadevan, Physica B 405 (2010) 3907.
[41] C. Justin Raj, S. Dinakaran, S. Krishnan, B. Milton Boaz, R. Robert, S. Jerome Das, Opt. Commun. 281 (2008) 2285.
[42] V.N. Joshi, Photoconductivity, Marcel Dekkar, New York, 1990.
[43] S. Karan, S. Sen Gupta, S. Prasad Sen Gupta, Mater. Chem. Phys. 69 (2001) 143.
[44] E.M. Onitsch, Mikroscopia 2 (1947) 131.
[45] M. Hanneman, Metall. Manch. 23 (1941) 135.
[46] S.K. Kurtz, T.T. Perry, J. Appl. Phys. 39 (1968) 3798.